

Dynamic transition in deposition with a poisoning species

F. D. A. Araújo Reis

*Instituto de Física, Universidade Federal Fluminense,
Avenida Litorânea s/n, 24210-340 Niterói RJ, Brazil*

(October 31, 2018)

In deposition with a poisoning species, we show that the transition to a blocked or pinned phase may be viewed as an absorbing transition in the directed percolation (*DP*) class. We consider a ballistic-like deposition model with an active and an inactive species that represents its basic features and exhibits a transition from a growing phase to a blocked or pinned phase, with the deposition rate as the order parameter. In the growing phase, the interface width shows a crossover from the critical $W \sim t$ behavior to Kardar-Parisi-Zhang (*KPZ*) scaling, which involves *DP* and *KPZ* exponents in the saturation regime. In the pinned phase, the maximum heights and widths scale as $H_s \sim W_s \sim (p - p_c)^{-\nu_{\parallel}}$. The robustness of the *DP* class suggests investigations in real systems.

PACS numbers: 05.50.+q, 64.60.Ht, 68.35.Ct, 68.55.Ln, 81.15.Aa

During some deposition processes, the presence of different chemical species improves films' properties but may also lead to undesired features, such as the decrease of growth rates due to erosion processes or the saturation of dangling bonds at the surface. One important example is the deposition of *Si* films doped with *P* by *CVD* or *MBE* in atmospheres with phosphine [1–3], in which it is observed the decrease of growth rates when phosphine flux increases. This feature seems to be related to the saturation of dangling bonds at the surface [3]. Similar poisoning effect appears in diamond *CVD* in atmospheres with boron and nitrogen [4]. High fluxes of the poisoning species may cancel out the growth of the main species, thus showing a transition from a growing phase to a blocked or pinned phase. Here we will argue that, in the absence of erosion processes of these two species, it may be viewed as a transition to an absorbing state in the directed percolation (*DP*) class [5–8], and we will present a deposition model that represents the main features of this process.

We will consider a statistical model that represents the essential aspects of films' growth and may be used to calculate growth rates, analyse surface roughness scaling and predict a dynamic transition. It is a ballistic-like deposition model with two species, an active one (*A*) and an inactive one (*B*), with a continuous transition from a growth phase to a blocked phase. The mapping of this transition onto the *DP* class shows that the growth velocity is the order parameter of the problem and that the growth phase corresponds to the active phase of *DP*. Thus their physical properties are completely different from previous models of surface growth with pinning or roughening transitions [9–13]. The observed fall of deposition rates in the growth regime agrees qualitatively with deposition experiments showing poisoning effects. Thus, the interpretation of the pinning process as a transition to an absorbing state and the robustness of the *DP* class strongly suggest that other transitions to blocked phases due to poisoning of films' growth are also in the *DP* class.

Furthermore, we will show that the scaling of quantities such as growth rates, surface roughness and thicknesses of blocked deposits involve the exponents of the Kardar-Parisi-Zhang (*KPZ*) theory [14] and *DP* exponents, and may eventually be used to compare our theory with experimental data.

In the following we will describe our model, show the results in one-dimensional substrates while discussing the relation to *DP*, show some results in two dimensions and present a final discussion.

In our model, particles *A* and *B* are released from random positions above a *d*-dimensional surface of length *L* with probabilities $1 - p$ and p , respectively. The incident particle follows a straight vertical trajectory towards the surface. Aggregation is allowed only if the incident particle encounters a particle *A* at the top of the column of incidence or at the top of a higher neighboring column. Otherwise the aggregation attempt is rejected. Fig. 1a illustrates the aggregation rules. A column in which aggregation is possible will be called an active column. The deposition time is the number of deposition attempts per substrate column, thus the deposition rate (number of deposited particles per unit time) is equal to the fraction of active columns.

It is clear from Fig. 1a that particles *B* represent impurities that prevent the growth to occur in their neighborhoods. This model resembles the *AC* model proposed by other authors [15,16], but their results are very different from ours (a morphological transition was suggested in $d = 2$ [16], but it was not quantitatively studied). Our findings are also completely different from the two-species *RSOS* model of Ref. [17], although the pure case ($p = 0$) also obeyed *KPZ* scaling.

Now we will present results in $d = 1$.

For small values of p , the growth process continues indefinitely, such as in the pure model ($p = 0$). However, when p increases, the growth rate r decreases due to the increase in the density of *B* at the surface, as shown in Fig. 2a. In Fig. 2b we show $\ln r$ versus $\ln(p_c - p)$ for

$p_c = 0.20715$, which gives the best linear fit of the data for $0.19 < p < 0.206$. Thus we obtain

$$r \sim \epsilon^\beta, \epsilon \equiv p_c - p, \quad (1)$$

with $p_c = 0.20715 \pm 0.00010$ and $\beta = 0.282 \pm 0.012$.

The instantaneous growth rate decays as the density of particles A at the surface. Focusing on the surface configuration, we notice that the growth rules of Fig. 1a may be mapped onto a d -dimensional contact process [18,7] (CP) in which a top A represents a particle and a top B represents a hole (or empty site), as shown in Fig. 1b. When the deposition of a B occurs in a column with a top A , it corresponds to the annihilation of a particle in the CP . On the other hand, the deposition of an A in a column with a top B and a neighboring column with a top A corresponds to offspring production in the CP . Notice that the stability of the absorbing state is represented by process 4 in Fig. 1b. The probabilities of annihilation and offspring production in the CP are not trivially related to p , since they also depend on the neighboring heights' distribution.

The equivalence to a CP indicates that the transition is in the DP class, with the density of top A or the growth rate r as the order parameter. The above value of the exponent β and forward results support this statement (the best known estimate for DP is $\beta = 0.276486 \pm 0.000008$ [19]).

Here it is relevant to recall that all known statistical models showing continuous transitions to absorbing states, with positive one-component order parameters, short-range interactions and no additional symmetries, are in the DP class [8,20]. This so called *robustness* of the DP class is the reason for us to expect universality in real systems' transitions with the same blocking mechanisms of our model.

At the critical point in $d = 1$ and $L \leq 8192$, we estimated the deposition rate at very long times, $r_\infty(L)$, and obtained

$$r_c(L, t = \infty) \sim L^{-\gamma}, \quad (2)$$

with $\gamma = 0.26 \pm 0.02$. This result is consistent with the expected DP value $\gamma = \beta/\nu_\perp$ (the best known estimate $\nu_\perp = 1.096854 \pm 0.000004$ [19] gives $\alpha \approx 0.252$). We also estimated r for relatively short times in very large substrates ($L = 65536$), and obtained

$$r_c(L = \infty, t) \sim t^{-\eta}, \quad (3)$$

with $\eta = 0.160 \pm 0.005$. This estimate also supports the DP equivalence, which gives $\eta = \beta/\nu_\parallel$, where ν_\parallel is the parallel correlation length exponent (best known estimate $\nu_\parallel = 1.733847 \pm 0.000006$ [19]).

The interface width, defined as

$$W(L, t) = \left[\left\langle \frac{1}{L^d} \sum_i (h_i - \bar{h})^2 \right\rangle \right]^{1/2}, \quad (4)$$

obeys dynamic scaling involving exponents of DP and KPZ theory (overbars and angular brackets in Eq. 3 denote spatial and configurational averages, respectively). In order to understand its behavior below the critical point, we first show the results at p_c and very large substrates in Fig. 3. The interface width W increases as

$$W \sim t, p = p_c, \quad (5)$$

as a consequence of the finite fraction of growing columns in isolated branches and the increasing fraction of blocked columns, which give rise to increasingly large heights' differences.

The evolution of the interface width for $p \lesssim p_c$ is presented in Fig. 4, where we plotted $\ln W$ as a function of the scaling variable $x \equiv t\epsilon^{\nu_\parallel}$, with $\nu_\parallel = 1.733847$ [19], in substrates with $L = 4096$. There is a transient region for $t < t_{cross} \sim \epsilon^{-\nu_\parallel}$, in which W shows the rapid increase typical of the critical point (Eq. 5). Notice that t_{cross} is the characteristic time of correlations in the DP process. At $t \sim t_{cross}$, W crosses over to a KPZ scaling

$$W \sim t^{\beta_K} \quad (6)$$

with $\beta_K = 1/3$ in $d = 1$. Finite-size effects are responsible for the reduced declivities in Fig. 4 when compared to the asymptotic forms of Eqs. (5) and (6) (strong finite-size effects are typical of ballistic deposition models [21]).

For long times, finite-size effects lead to the saturation of the interface width. The extrapolation of data for several p and L , also considering finite-size effects [21], leads to

$$W_{sat} \sim \epsilon^{-\beta} L^{\alpha_K}, \epsilon \ll 1, L \gg 1, \quad (7)$$

with the KPZ exponent $\alpha_K = 1/2$ and the DP exponent. $\epsilon^{-\beta}$ is the typical lateral distance between active columns, but appears in Eq. (4) as a vertical scaling length, accounting for lateral correlations in the roughness saturation regime. The divergence of W_{sat} at p_c indicates the failure of KPZ scaling at criticality.

For $p > p_c$, the growth process stops when the whole surface is covered with B , for any length L . The heights of the blocked deposits attain limiting or saturation values with average H_s , and the interface widths attain saturation values W_s (W_s should not be confused with W_{sat} for $p < p_c$, since the former is a property of infinitely large static deposits and the latter is related to finite-size effects in growing deposits). The time for surface blocking is the characteristic time of survival of particles in the corresponding CP , consequently H_s and W_s should behave as the parallel correlation length in the absorbing phase:

$$H_s \sim W_s \sim (-\epsilon)^{-\nu_\parallel}. \quad (8)$$

Eq. (8) is confirmed in Fig.5, where we show linear fits of $\ln H_s$ and $\ln W_s$ versus $\log(-\epsilon)$, with $p_c = 0.20715$ (the same estimate of the growing phase). From fits with

different values of p_c we obtain $\nu_{\parallel} = 1.75 \pm 0.05$, which is also consistent with DP within error bars [19].

Analogous results were obtained in two-dimensional substrates. In Fig. 6a we show $\log r$ versus $\log \epsilon$, with $p_c = 0.4902$, which gives $\beta = 0.573 \pm 0.020$ (Eq. 3). In Fig. 6b we show $\ln W$ versus $\ln x$, $x \equiv t\epsilon^{\nu_{\parallel}}$, for several values of p , considering $\nu_{\parallel} = 1.295$ [22]. Again it shows exponents consistent with DP and the crossover from DP to KPZ scaling. At $p = p_c$ we obtained Eq. (5) with $\alpha \approx 0.46$, to be compared with the DP value $\alpha \approx 0.451$ [22]. The results in $d = 2$ are less accurate due to the limitations in lattice lengths ($L \leq 256$), but are essential to justify any comparison of our theory with experiments.

The applicability of our model to real growth processes is limited due to the ballistic aggregation conditions, the absence of diffusion mechanisms etc. However, if poisoning effects lead to a transition to a blocked phase and if it can be interpreted as a transition to an absorbing phase, then the robustness of the DP class [20,8] suggests this type of transition. A possible realization is Si deposition in atmospheres with phosphine (PH_3), which shows a decrease of growth rate with increasing phosphine flux. The saturation of phosphorous dangling bonds by hydrogen at the surface was suggested as the main blocking mechanism [3], but to our knowledge no blocking transition was found yet. Another possible application is diamond CVD in atmospheres with boron, in which the formation of an amorphous BCN phase blocks the growth of the diamond phase for boron to carbon ratios above $B/C = 0.1$ [4]. It seems to be an absorbing transition similar to our model and, consequently, is a candidate to the DP class.

Finally, it is important to recall the differences between the transition found in our model and the pinning transitions by directed percolation of growing interfaces in disordered media [9,10,23,8]. In that case the interface is blocked if the impurity concentration exceeds the DP threshold, then infinite surface growth is found in the absorbing phase of the impurities system. Consequently, the critical behavior of geometric quantities such as growth rate and interface width are completely different; for instance, Eq. (3) is obeyed with $\beta = \nu_{\parallel} - \nu_{\perp}$ [23]. A very different correspondence to DP is also found in models with competition between aggregation and desorption that show roughening transitions [11], in which the film growth regime parallels the absorbing DP phase.

ACKNOWLEDGMENTS

The author thanks Dr. Dante Franceschini for useful suggestions and helpful discussions. This work was partially supported by CNPq and FAPERJ (Brazilian agencies).

- [1] K. Verner et al, J. Crystal Growth **164**, 223 (1996).
- [2] C. Li et al, J. Vac. Sci. Technol. A **14**, 170 (1996).
- [3] F. Gao et al, J. Crystal Growth **220**, 461 (2000).
- [4] J. H. Edgar, Z. Y. Xie and D. N. Braski, Diamond Relat. Mater. **7**, 35 (1998).
- [5] S. R. Broadbent and J. M. Hammersley, Proc. Camb. Phil. Soc. **53**, 629 (1957).
- [6] W. Kinzel, Z. Phys. B **58**, 229 (1985).
- [7] J. Marro and R. Dickman, *Nonequilibrium Phase Transitions in Lattice Models* (Cambridge University Press, Cambridge, 1999).
- [8] H. Hinrichsen, Adv. Phys. **49**, 815 (2000).
- [9] S. V. Buldyrev et al, Phys. Rev. A **45**, R8313 (1992).
- [10] L.-H. Tang and H. Leschhorn, Phys. Rev. A **45**, R8309 (1992).
- [11] U. Alon et al, Phys. Rev. Lett. **76**, 2746 (1996); Phys. Rev. E **57**, 4997 (1998).
- [12] H. Hinrichsen et al, Phys. Rev. Lett. **79**, 2710 (1997).
- [13] S. Park and B. Kahng, Phys. Rev. E **60**, 6160 (1999).
- [14] M. Kardar, G. Parisi and Y.-C. Zhang, Phys. Rev. Lett. **56**, 889 (1986).
- [15] W. Wang and H. A. Cerdeira, Phys. Rev. E **47**, 3357 (1993).
- [16] H. F. El-Nashar, W. Wang, and H. A. Cerdeira, J. Phys. Condens. Matter **8**, 3271 (1996).
- [17] S. S. Botelho and F. D. A. Aarão Reis, Phys. Rev. E **65**, art. no. 032101 (2002).
- [18] T. E. Harris, Ann. Prob. **2**, 969 (1974).
- [19] I. Jensen, J. Phys. A **32**, 5233 (1999).
- [20] H. K. Janssen Z. Phys. B **42**, 151 (1981); P. Grassberger, Z. Phys. B **47**, 365 (1982).
- [21] F. D. A. Aarão Reis, Phys. Rev. E **63**, art. no. 056116 (2001).
- [22] C. A. Voigt and R. M. Ziff, Phys. Rev. E **56**, R6241 (1997).
- [23] A.-L. Barabási and H. E. Stanley, *Fractal Concepts in Surface Growth* (Cambridge University Press, New York, 1995).

FIG. 1. (a) Examples of deposition attempts in $d = 1$, in which only the configurations of the incident column and of neighboring columns are shown. Open squares represent particles A , filled squares represent particles B and crossed squares represent incident particles (A or B). In processes (1), (2) and (3), aggregation occurs at the positions marked with a filled circle. In processes (4) and (5) the aggregation attempt is rejected. Notice that, in processes (3) and (4), lateral aggregation to the right is not possible because the neighboring A is not at the top of the column. (b) The equivalent one-dimensional contact process, in which a top A corresponds to a particle (empty circles) and a top B corresponds to a hole (underlined empty site). The initial configuration and the possible final configurations (for the cases of incident A or incident B) are shown.

FIG. 2. (a) Deposition rate r versus probability p of incidence of particles B , in $d = 1$. (b) Scaling of r near $p_c = 0.20715$.

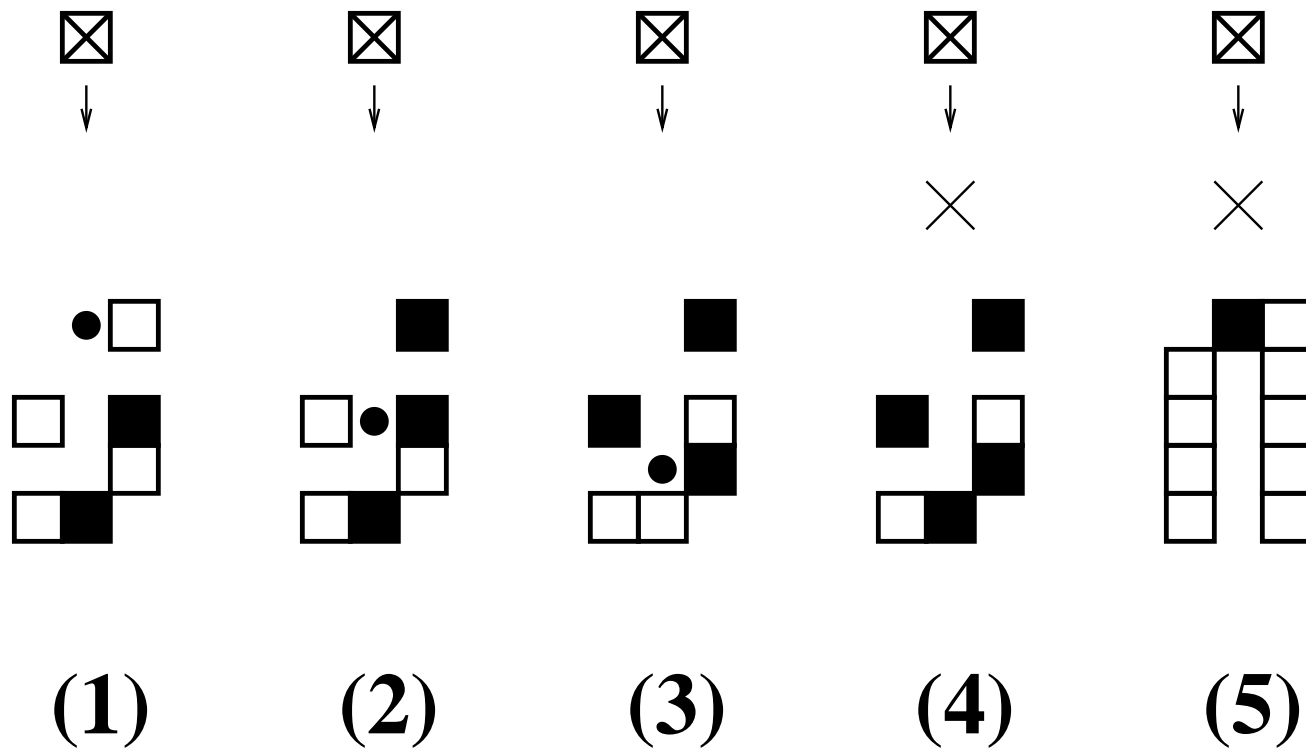
FIG. 3. Time evolution of the interface width W at the critical point $p_c = 0.20715$ in $d = 1$, for a very large substrate ($L = 65536$).

FIG. 4. $\ln(W)$ versus $\ln(x)$, with the scaling variable $x \equiv t\epsilon^{\nu_{\parallel}}$. From below to above, $p = 0.15$, $p = 0.17$ and $p = 0.18$ ($L = 4096$). The regions of critical DP and KPZ behaviors are indicated.

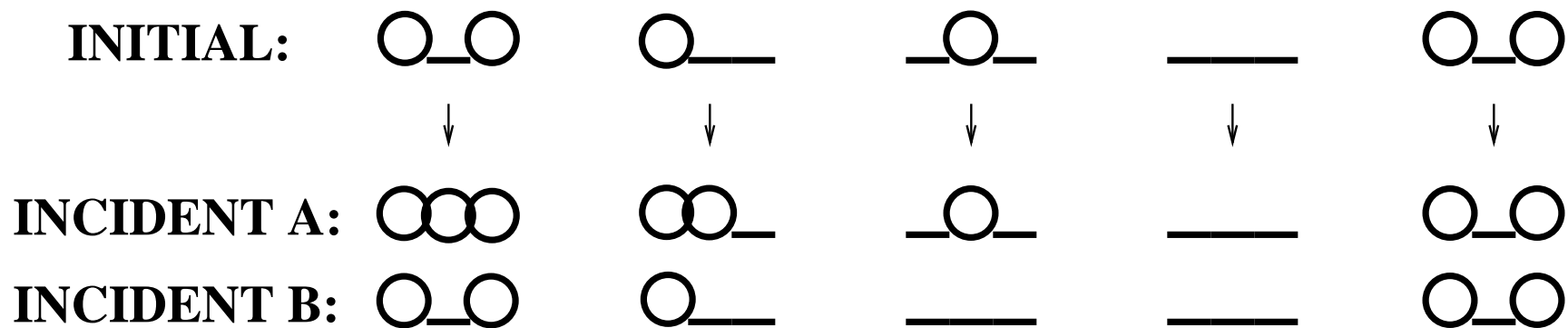
FIG. 5. Saturation height $\ln(H_s)$ (squares) and saturation width $\ln(W_s)$ (crosses) versus $\ln(-\epsilon)$ in $d = 1$, with $p_c = 0.20715$. The solid line is a least squares fit of H_s data, giving a declivity $\nu_{\parallel} \approx 1.75$.

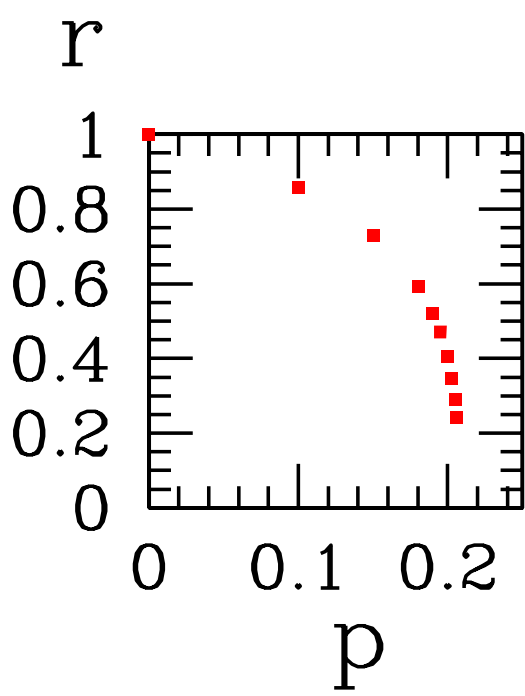
FIG. 6. (a) Scaling of the deposition rate r near $p_c = 0.4902$ in $d = 2$, giving $\beta = 0.573$. (b) $\ln(W)$ versus $\ln(x)$, with $x \equiv t\epsilon^{\nu_{\parallel}}$, for $p = 0.44$, $p = 0.46$ and $p = 0.47$ from below to above ($L = 256$).

(a)

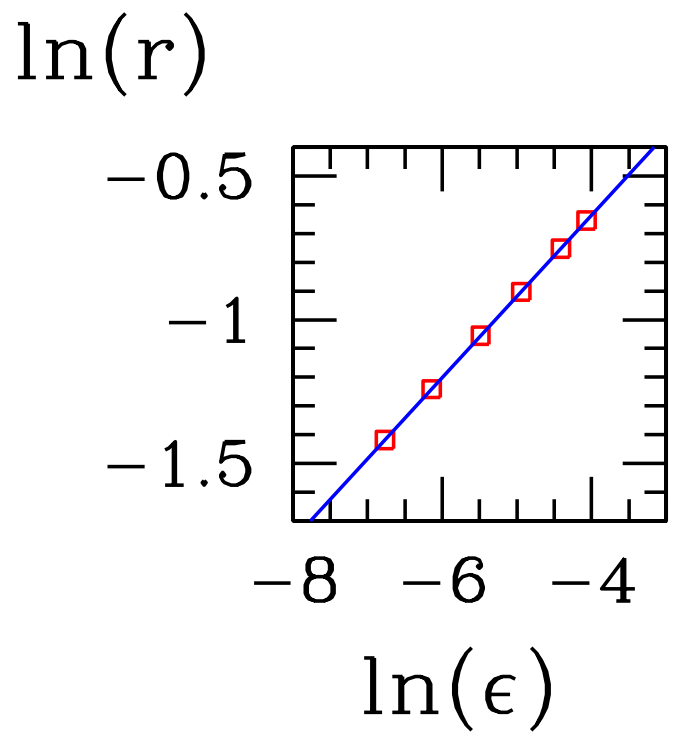


(b)

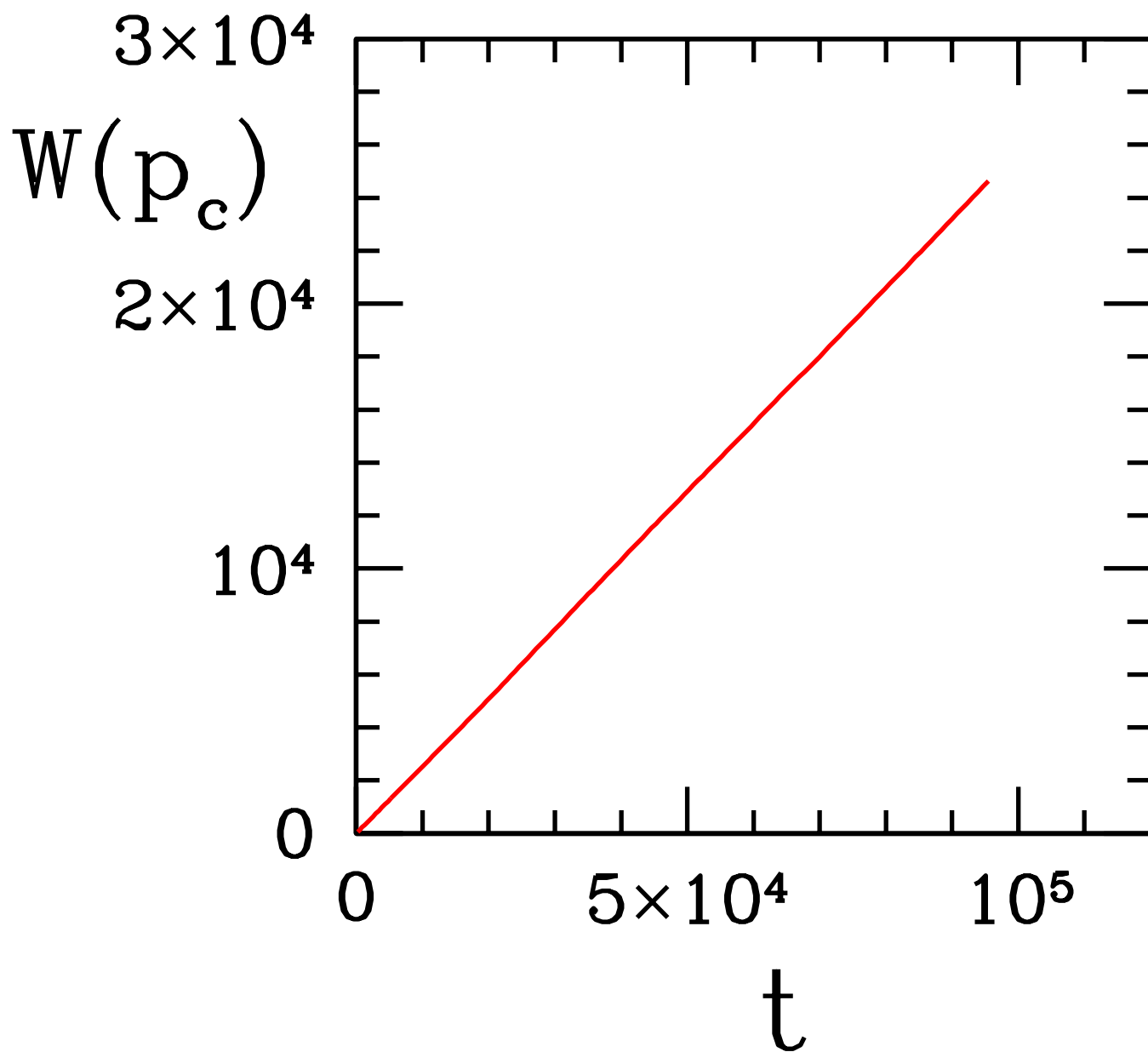


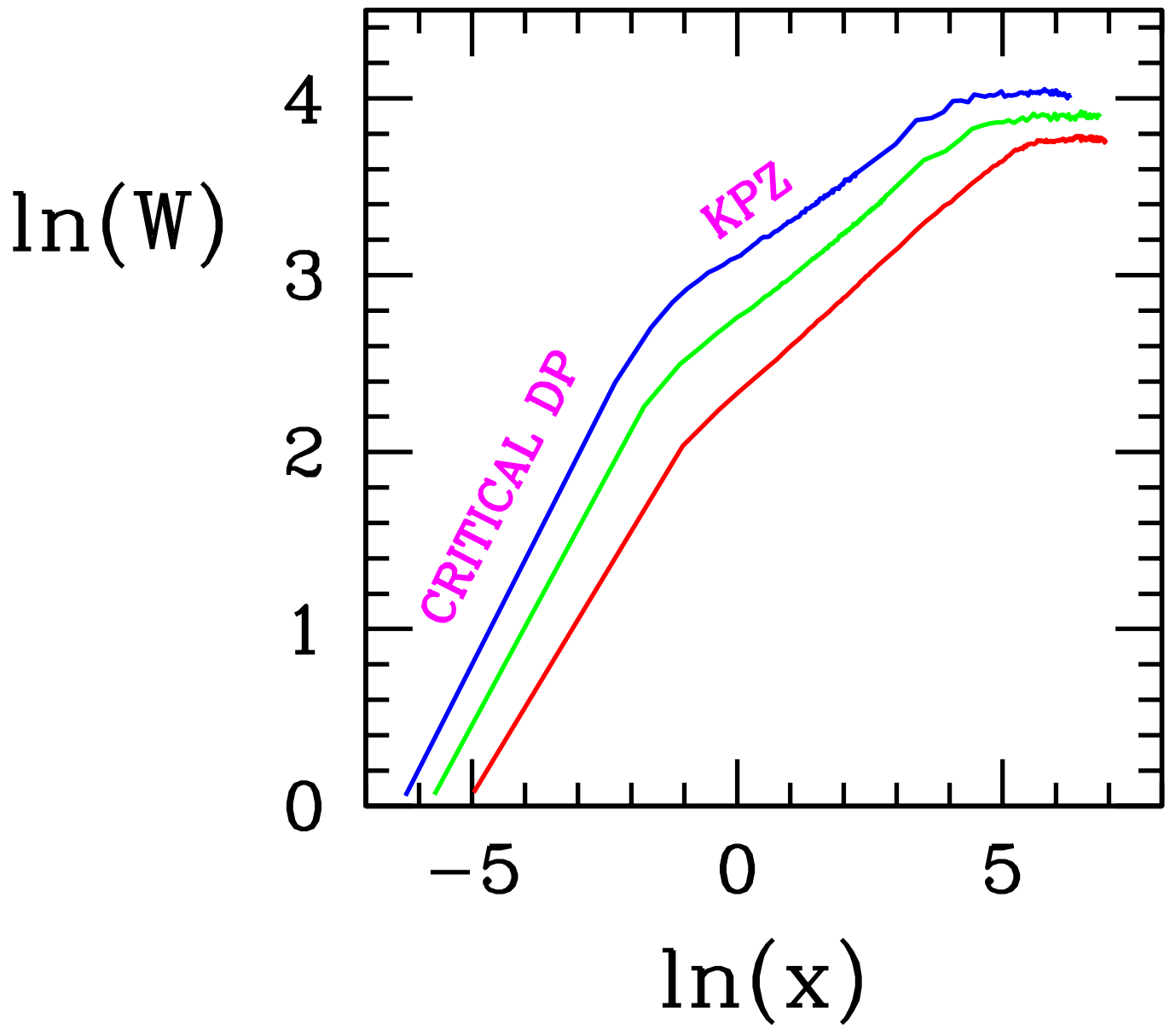


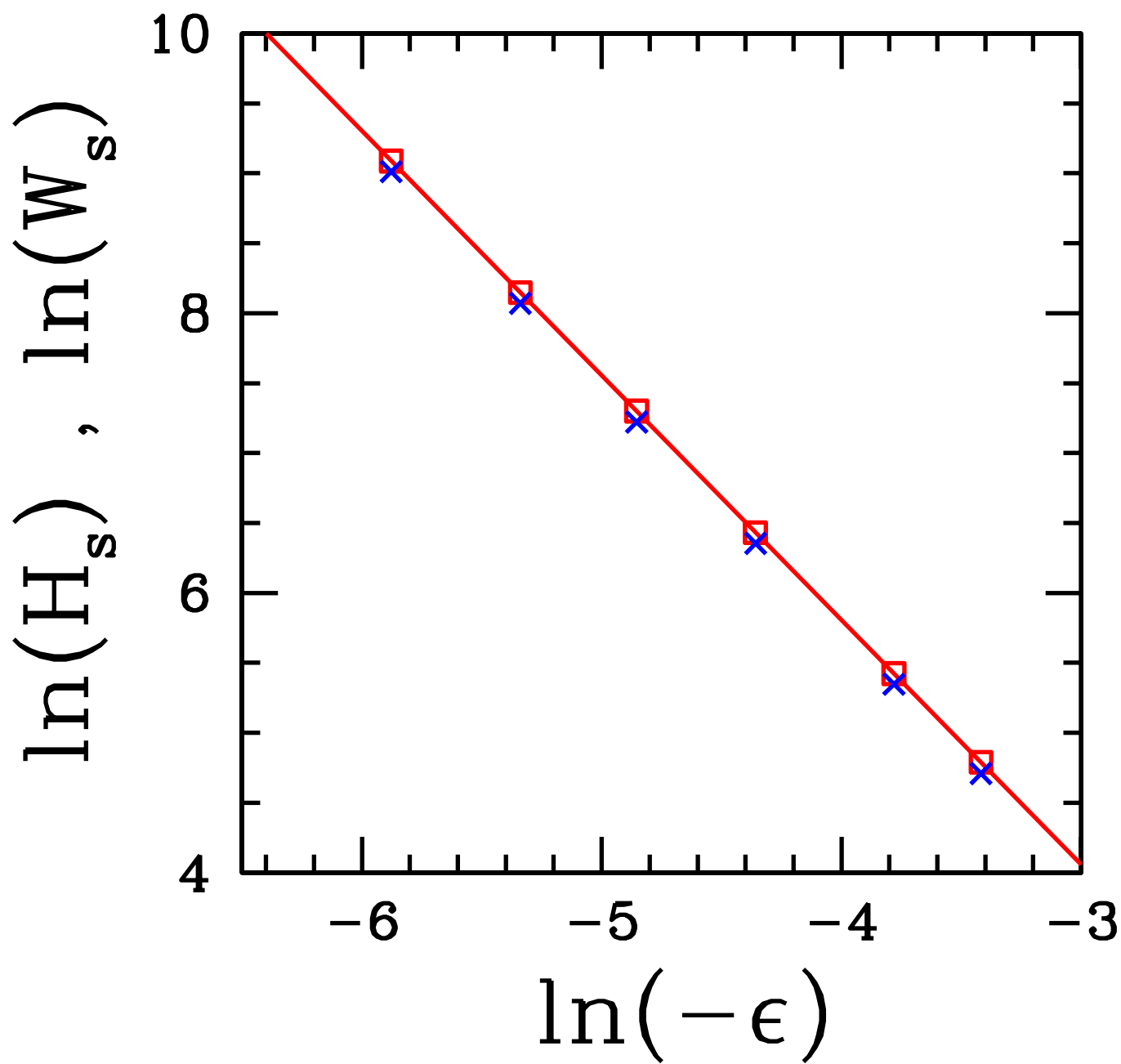
(a)

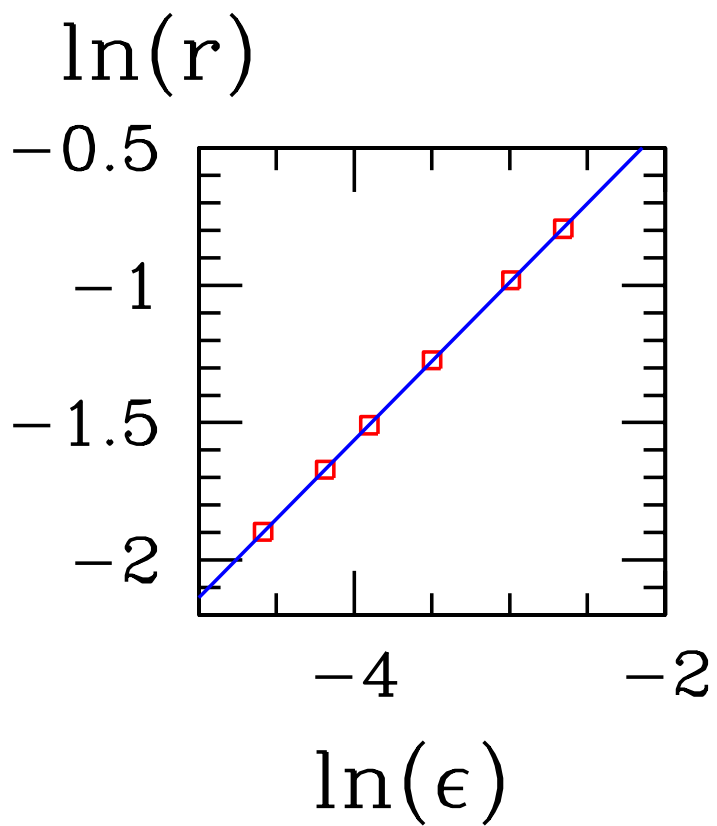


(b)

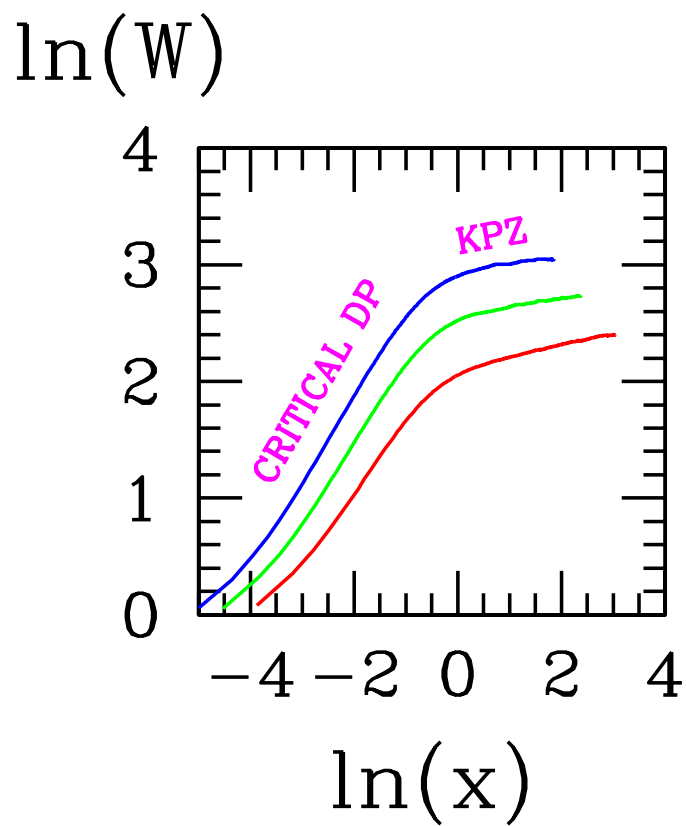








(a)



(b)